Front. Earth Sci. 2021, 15(3): 543–552
https://doi.org/10.1007/s11707-021-0896-7

RESEARCH ARTICLE

UAV-based spatial pattern of three-dimensional green volume and its influencing factors in Lingang New City in Shanghai, China

Sijun ZHENG[1,2], Chen MENG[3,4], Jianhui XUE (✉)[1], Yongbo WU[1], Jing LIANG[2], Liang XIN[5], Lang ZHANG[2]

1 College of Biology and the Environment, Nanjing Forestry University, Nanjing 210037, China
2 Shanghai Academy of Landscape Architecture Science and Planning, Shanghai 200241, China
3 School of Ecological and Environmental Sciences, East China Normal University, Shanghai 200241, China
4 Shanghai Key Laboratory for Urban Ecological Processes and Eco-Restoration, Shanghai 200241, China
5 Shanghai Institute of Surveying and Mapping, Shanghai 200063, China

Abstract Three-dimensional green volume (TDGV) reflects the quality and quantity of urban green space and its provision of ecosystem services; therefore, its spatial pattern and the underlying influential factors play important roles in urban planning and management. However, little is known about the factors contributing to the spatial pattern of TDGV. In this paper, TDGV and land use intensity (LUI) extracted from high spatial resolution (0.05 m) remotely sensed data acquired by an unmanned aerial vehicle (UAV), anthropogenic factors[1)] and natural factors[2)] were utilized to identify the spatial pattern of TDGV and the potential influencing factors in Lingang New City, a rapidly developed coastal town in Shanghai. The results showed that most of the TDGV was distributed in the western part of this new city and that its spatial variations were significantly axial. TDGV corresponded well with the chronologies of land formation, urban planning, and construction in the city. Generalized least squares (GLS) analysis of TDGV (grid cell size: 100 × 100 m) and its influencing factors showed that the TDGV in this new city was significantly negatively correlated with both LUI and distance from roads and significantly positively correlated with land formation time and distance from water. Distance from buildings did not affect TDGV. Additionally, the degree of influence decreased in the following order: distance from water > land formation time > distance from roads > LUI. These results indicate that the spatial pattern of TDGV in this new town was mainly affected by natural factors (i.e., the distance from water and land formation time) and that the artificial disturbances caused by rapid urbanization did not decrease the regional TDGV. The main factors shaping the spatial distribution of TDGV in this city were local natural factors. Our findings suggest that the improvement in local soil and water conditions should be emphasized in the construction of new cities in coastal areas to ensure the efficient provision of ecological services by urban green spaces.

Keywords low-altitude remote sensing, LUI, urban space layout, land formation time, dominant factor

1 Introduction

Approximately one-third of the world's population lives in coastal regions characterized by rapid urbanization. Land resources are the basis for urban development; thus, surrounding the sea and reclaiming land from the sea are important means by which coastal cities can expand their development space. Some examples include sea reclamation for salt production on the eastern coast of China in the 1950s, for farmland around the 1970s, for aquaculture around the 1990s, for the construction of coastal new cities or industrial zones in approximately 2000 (Li and Yu, 2013; Gao et al., 2014), and for the construction of new cities or land in the San Francisco Bay area in the USA and in Tokyo Bay in Japan. In the past 50 years, coastal areas worldwide have experienced the expansion of urban functional districts and the construction of new cities or industrial zones. The land space for these areas has been

Received November 9, 2020; accepted March 22, 2021

E-mail: jhxue@njfu.com.cn

1) LUI, Distance from buildings and Distance from roads.
2) Land formation time and Distance from water.

obtained mainly through artificial land formation, such as Japan's Tokyo Haneda International Airport, China's Shanghai Lingang New City and Tianjin Binhai New Area, reclamation from lakes for the United States' northern San Francisco Bay, and the Netherlands' Zuider Zee Project. However, the ecotone between sea and land is an important ecological buffer zone, ecological resource belt and biological habitat, and its functions can be seriously damaged after the artificial acceleration of land resources or the building of embankments for land formation; the rapid urbanization of coastal areas and the replacement of their natural siltation have become the norm (Zhang et al., 2015; Çetin, 2016; Yaralioğlu and Ozden, 2019). The large-scale rapid urbanization and industrialization of coastal regions have transformed these areas into new land-based urban areas with a complex blend of ecology, human life and production. Given the challenges of responding to the transformation of new sustainable development models for cities (i.e., low-carbon cities, resilient cities and eco-cities), the model of coastal city construction must also consider how to coordinate the relationship between human construction activities and the natural conditions in coastal areas to promote the sustainable development of new coastal land-based areas.

The concept of three-dimensional green volume (TDGV) originated from the concept of the leaf area index (LAI). TDGV is based on the area or volume of plant leaves and stems, which can indicate the status of plant growth and development and consequently the functioning of plant ecosystem services at the individual and population levels. With the development of satellite remote sensing, starting in the 1990s, new indices (i.e., green volume, TDGV, and green plot volume) have been proposed to evaluate the quality of urban green space, urban forests, and urban environments; these proposals have led to a shift in the evaluation of urban ecological space from two to three dimensions (Zhou, 2001; Zhou and Zhou, 2001; Gregg et al., 2003; Ong, 2003; Zhou and Zhou, 2006; Anderson et al., 2018; Li et al., 2008; Zhou et al., 2015; Zhou et al., 2016). In recent years, the mature application of low-altitude unmanned aerial vehicles (UAVs) has further improved the accuracy of TDGV extraction and analysis. Lingang New City is a typical example of the rapid urbanization and construction in China's coastal areas in recent years; from the start of its planning, this city was based on the concept of a low-carbon eco-city, with a focus on the construction of urban green ecological spaces and landscapes (Sun, 2011). In this study, an evaluation and feature analysis of the TDGV in the central area of Lingang New City was conducted using low-altitude remote sensing by a UAV. The goals of this study were to analyze the relationships between the ecological landscape features represented by TDGV and land formation time, water distribution, and human disturbances (i.e., land use intensity (LUI) and urban space layout) and to identify the main factors affecting the quality of the urban ecological environment during the rapid urbanization in this new coastal city. The results can guide the planning, construction and management of new cities built on land reclaimed from the sea.

2 Data and methods

2.1 Study area

Shanghai is located at the intersection of the coastline and the Yangtze River Estuary, China (30°40′–31°53′N, 120°51′–122°12′E). Its coastal area is composed of the south bank of the Yangtze River, the surrounding islands and the northern shore belt of Hangzhou Bay. The vast majority of the Shanghai coastline is a muddy coast. Lingang New City is located at the south-eastern tip of Shanghai. To the west of the city is Nanhui Luchaogang Harbour, to the east is the East China Sea, and to the south are Putong Mountain, Shengsi Island, and the large and small Yangshan Islands. The city is approximately 50 km from the urban area of Shanghai, and its planned area is 296.6 km^2, of which 30% derives from sea reclamation. The project started in 2001 and was officially launched on November 30, 2003. Lingang New City is positioned as a highly coordinated, fully functional and vibrant integrated coastal new city and is a strategic focus area with the status of an auxiliary city to Shanghai (Fig. 1). The target area in this work is the central area of the master plan for Lingang New City (Shanghai urban planning and design reasearch institute, 2009; Liu et al., 2012). In recent years, with the construction of the Waigaoqiao port of Pudong New District, the expansion of Pudong Airport, the construction of the Yangshan International Deepwater Port and the development of the Jinshan industrial zone, the land use and landscapes in the Shanghai coastal zone have undergone drastic changes. Furthermore, Shanghai continues to promote deposition and conduct reclamation in the coastal zone, which could provide land resource reserves for urban development. These phenomena will have far-reaching impacts on the entire coastal belt and surrounding areas.

2.2 Layout of transect belts and samples

Dishui Lake is the center of the layout and first in the constructions sequence planned for Lingang New City according to its urban planning layout. We identified eight transect belts (45° angle) with Dishui Lake as the center: north (N) (vertical line), north-east (NE), east (E) (horizontal line), south-east (SE), south (S) (vertical line), south-west (SW), west (W) (horizontal line), and north-west (NW) (Fig. 2). For each transect belt, we defined Dishui Lake as zero, and the number of sample grids (500 m× 500 m) from the lake to the boundary of the coverage area was determined (Fig. 1). The data from these sample grids were used for the analysis of the axial trends

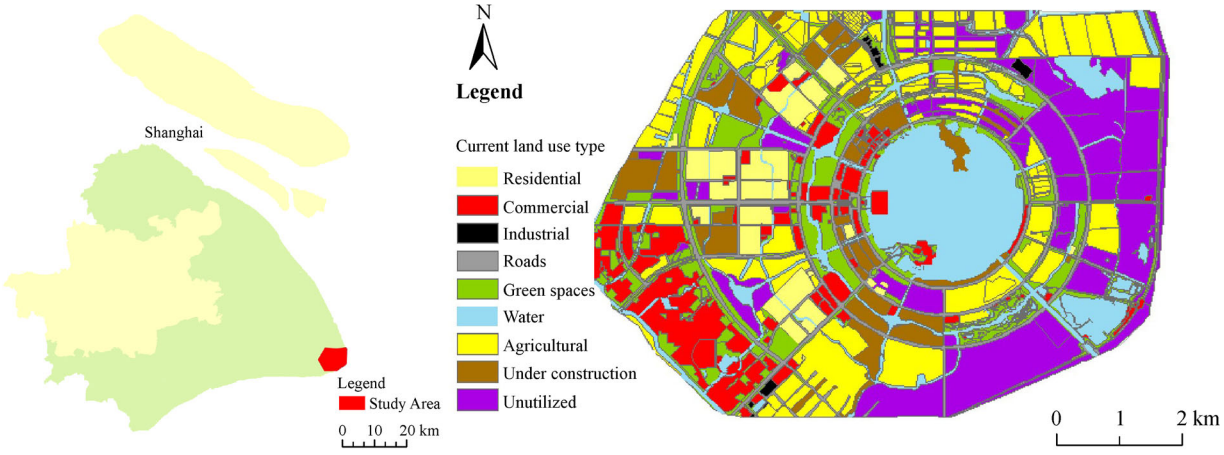

Fig. 1 Location of Shanghai Lingang New City and its coverage of different land use types.

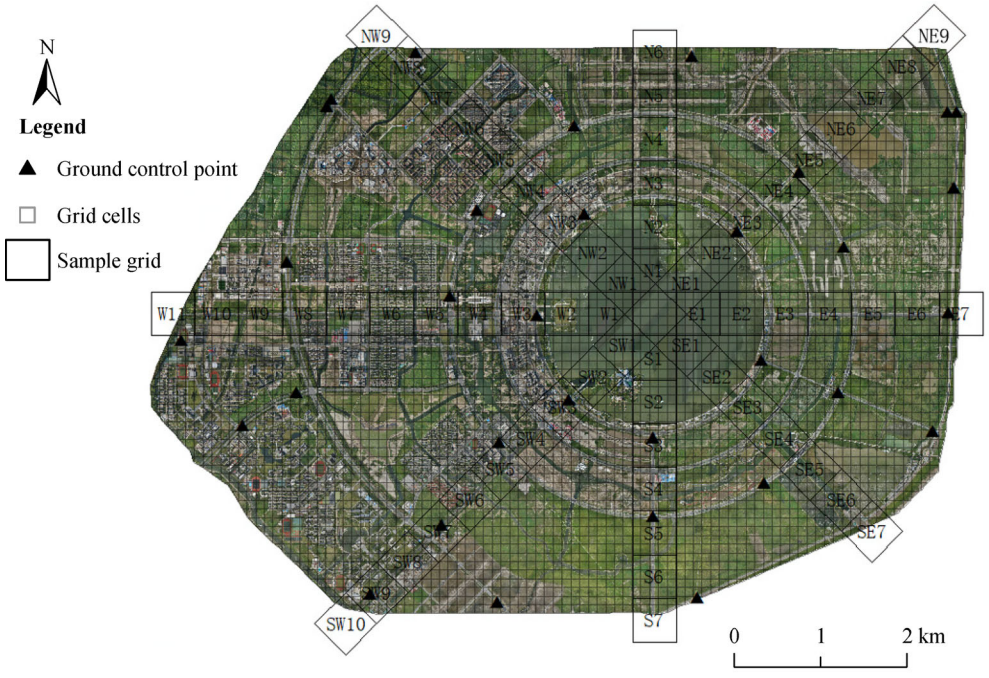

Fig. 2 Layout of transect belts, grid cells, and ground control points. Each sample grid in each transect belt was numbered in order (E1-E7, W1-W11, N1-N6, S1-S7, SE1-SE7, NE1-NE9, NW1-NW9, and SW1-SW10) with Dishui Lake at the center.

in TDGV. In addition, the study area was divided into grid cells (100 m× 100 m), yielding a total of 5187 cells, and the indices (i.e., TDGV; distances from buildings, roads and water; and LUI) for each cell were calculated for the subsequent analysis of influencing factors.

2.3 Data acquisition by UAVs

2.3.1 Image acquisition

On July 27, 2018, a UAV flight with 10 vehicles (255 m high) covered approximately 50.75 km^2, and a total of 11,342 images were taken using a Sony 5100 camera (0.05 m resolution). Thirty-three ground control points (GCPs) were collected with a Trimble R2 receiver, USA. Aerial triangulation was conducted using PHOTOMOD software, and a digital surface model (DSM, 0.1 m resolution), digital elevation model (DEM, 0.1 m resolution) and orthographic images (0.1 m resolution) were consequently produced.

2.3.2 Basic parameters of aerial photography

The main route flight direction was east–west, and the

perpendicular direction was north–south. The coordinate system employed was WGS 1984 UTM Zone 51°N. The flight height was 255 m, and the overlap of images was 80% in the main flight direction and 60% in the side direction. The ground resolution was 0.05 m. The total photographed area was 50.63 km^2(Fig. 3).

2.3.3 Collection of GCPs

Thirty-three GCPs with obvious features that were distributed evenly across the whole image were collected by real-time kinematic (RTK) and differential GPS. These points were distributed at road intersections and sites with obvious contour boundaries. The projection coordinate system was UTM, and the geographic coordinate system was WGS1984.

2.4 Calculation of TDGV

Based on the DSM and DEM extracted using PHOTOMOD software, TDGV was calculated using the following equation:

$$V_c = \sum_{i=1}^{s}\sum_{j=1}^{t} \Delta d^2 |h_{ij} - H_{ij}|, \quad (1)$$

where V_c is the TDGV of vegetation; s and t are the line and column numbers, respectively, for the DSM; Δd is the length of the DSM grid; h_{ij} is the DSM elevation; and H_{ij} is the DEM elevation.

When calculating the TDGV of a treed area, the trunk part should be subtracted from the model of the heights of the trees and of the lowest leaves. Therefore, two vegetation regions were distinguished according to vegetation height (h_{ij}–H_{ij}): the tree area (height > 2 m) and the shrub or grass area (height < 2 m). Additionally, 13 samples (20 m× 20 m) were taken in treed areas, and further sample investigations were conducted. The heights of the trees and of the lowest leaves were *in situ* measured, and a correlation model for these parameters was constructed.

2.5 Integrative index of LUI

Based on the mapping and interpretation of the UAV orthophoto, six land use types in the region were classified: cultivated land, forestland, garden land, water body, construction land and unused/unsuitable land. In addition, four grades of LUI were determined: grade 1 was unused/unsuitable land, grade 2 was forestland/water (forestland, water body), grade 3 was agricultural land (cultivated land, garden land), and grade 4 was construction land (buildings, industrial, mining or transportation land).

The following equation was used to calculate LUI (Gao et al., 1999):

$$\text{Intensity}_x = \sum_{i=1}^{4} A_i \times S_i / S, \quad (2)$$

where Intensity_x is the LUI of sample grid x, A_i is grade i of LUI, S_i is the land area of grade i, and S is the total land area of the sample grid (Ong, 2003).

LUI was classified into five levels in this work: lowest use intensity (LUI < 125%), low use intensity (125% < LUI < 150%), moderate use intensity (150% < LUI < 175%), high use intensity (175% < LUI < 250%), and highest use intensity (LUI > 300%) (Ma et al., 2019).

2.6 Calculation of distances from roads, water and buildings

We obtained the road layer, water layer, and building layer based on the mapping and interpretation of the UAV orthophoto with 0.1 m resolution. The Euclidean distance

Fig. 3 Bird's eye view of Lingang New City from east to west.

of each sampled cell center to each pixel within roads, water, or buildings was calculated using the ArcGIS 10.6 Spatial Analyst module with the EucDistance function and then resampled with cells (100 m× 100 m); the mean Euclidean distance values of the cells were used for sampling. The equation employed for the calculation of Euclidean distance was as follows:

$$D = \sqrt{(\chi_2 - \chi_1)^2 + (\gamma_2 - \gamma_1)^2}, \quad (3)$$

where χ_2 and γ_2 are the center coordinates of the sample grid cells and χ_1 and γ_1 are the coordinates of pixels within the area of roads, water or buildings.

2.7 Statistics

The generalized least squares (GLS) method was used to analyze the effects of the parameters (i.e., LUI; distances from buildings (D_house), roads (D_road) and water (D_water); and land formation time (Land_Year)) on TDGV. In the model, we used the center coordinates of each cell to correct for the impact of spatial autocorrelation on the spatial pattern of the green volume and chose exponential spatial autocorrelation for the analysis based on the Akaike information criterion (AIC) values of the model. The analysis described above was performed in R software using the gls command function of the nlme software package.

3 Results and discussion

3.1 Spatial distribution patterns of TDGV in Lingang New City, Shanghai

Overall, the TDGV per unit area in Lingang New City was 0.46 m^3/m^2, and the total TDGV was 2135.07 million m^3. The proportions of patches with low (< 3000 m^3), medium (3000–9000 m^3), and high (> 9000 m^3) TDGV values were 64.8%, 21.4%, and 13.8%, respectively, and the TDGV in construction land and forestland/water accounted for most of the TDGV in this new city (Table 1).

The areas with high TDGV values were distributed mainly on the west side of Dishui Lake and were dominated by patches with medium TDGV values. A few patches with high TDGV values were also scattered throughout this area. Additionally, large variation in TDGV was evident on the west side of the lake; from west to east, TDGV first increased and then decreased, showing a U-shaped pattern with obvious directionality. Specifically, the TDGV values distributed in the boundary area of the west side, the area surrounding Dishui Lake, and the area adjacent to the main road were higher than those in the other areas. The overall TDGV was composed of largely homogenous patches, mainly patches with low TDGV values (Fig. 4).

The analysis of TDGV in the eight transect belts showed that the TDGV values in the west, north-west and south-west transect belts were significantly higher than those in the other five transect belts, and the TDGV values of most transect belts showed a U-shaped pattern (Fig. 5). The abovementioned areas with high TDGV values were largely consistent with the main functional area of the city center as described in the Lingang New City master plan, and the axial characteristics of TDGV were consistent with the regional development and construction timing (Sun, 2011).

TDGV was distributed mainly in the western, north-western, and south-western parts of the new city and showed a significant axial pattern with Dishui Lake as its axis. This pattern has some connection with the overall planning and development history of the Central District and its land formation time. These axial characteristics are consistent with the axial traits of the regional LUI, which indicates the regional axial development of human disturbances (Zhou et al., 2005; Wang and Liao, 2006).

3.2 Spatial patterns of TDGV in Lingang New City and the analysis of the factors underlying its formation

3.2.1 Spatial characteristics of the main influencing factors of TDGV in Lingang New City

The LUI in Lingang New City was 220%, which is high. Among the grades of LUI, forestland/water had the highest proportion, followed by construction land. The spatial variation in LUI in Lingang New City was obvious. With the north–south axis of Dishui Lake as the boundary, the LUI values in the western region were significantly higher than those in the eastern region, and LUI in the western region showed obvious axial changes from east to the west as well as multiple centers. Moreover, from west to east across the entire research area, LUI showed a gradual decreasing trend (Fig. 6).

The distances of most of the patches in Lingang New City from buildings, roads, or water were less than 500 m; the shortest distances were from buildings, and the longest distances were from roads. This latter result reflected the

Table 1 Area and TDGV of different land use types in Lingang New City. TDGV: three-dimensional green volume

	Unused/unsuitable land	Forestland/water	Agricultural land	Construction land
Area/m^2	11469617.14	131296354.60	10703716.95	17596630.30
TDGV/m^3	2704005.10	12563090.73	2847261.99	15863733.42
Proportion of TDGV/%	7.96	36.97	8.38	46.69

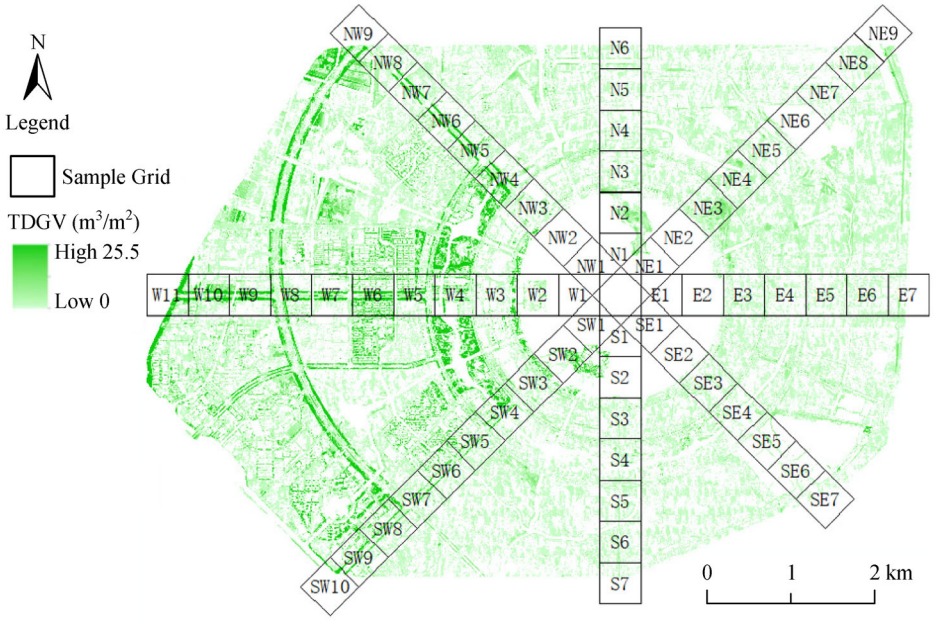

Fig. 4 Spatial distribution of three-dimensional green volume in Lingang New City, Shanghai.

high density of construction land due to its planning and layout as well as the emphasis on subsidiary ecological spaces (i.e., green spaces along roads, waterfront green space). The construction of dikes began in the mid-20th century to promote shoreline silting in this new city, beginning with Renmin Dike (1949), followed by Jiefang Dike (1974), 85 Dike (1983), 94 Dike (1994), and Shiji Dike (2002). The land formation from Renmin Seawall to 94 Dike occurred through natural siltation, and the land in Shiji Dike was formed via blow-filling technology for the construction of this new city (Fig. 7).

TDGV is a comprehensive index that reflects the quality of urban green space and the urban environment; it characterizes the spatial properties with which plants grow and develop at the individual and population levels and consequently perform regional ecosystem services (Li et al., 2008; Grafius et al., 2016; Casalegno et al., 2017). Therefore, the spatial pattern of urban TDGV is the result of the interactions of multiple factors (i.e., regional natural conditions, urban planning and layout, and urban construction management); however, its main controlling factors are still unclear (Fahmy et al., 2020). Lingang New City is a satellite city of Shanghai located on newly formed coastal land that has experienced rapid urbanization and city construction, and the urban spatial distribution of TDGV has been affected by both anthropogenic (i.e., regional land use, city layout) and natural (i.e., land formation time, water distribution) factors (Chen et al., 2003; Gong and Xia, 2006; Wang and Liao, 2006; Zhang et al., 2008; Chunwate et al., 2019; Han et al., 2020). Therefore, several influencing factors (LUI; distances of patches from buildings, roads and water; and land formation time) were investigated in this study.

3.2.2 Analysis of factors influencing the spatial distribution of TDGV in Lingang New City

GLS analysis with nlme spatial autocorrelation was used to test four models with different spatial structures (m1, m2, m3, and m4), and their fit and performance were evaluated by comparing their AIC values. The results were as follows: AIC (m1) 16009.32 > AIC (m2) 15898.72 > AIC (m3) 16091.63 > AIC (m4) 15896.73. We chose m4, which had the lowest AIC value, as the optimal model, and its correlation structure is exponential spatial correlation. Its equation was Log(green + 1) ~ LUI + Land_Year + log(D_water + 1) + log(D_road + 1) + log(D_house + 1), and its statistical parameters are shown in Table 2.

According to the optimal model analysis results (Table 3), TDGV in the sample cells (100 m × 100 m) was significantly negatively correlated with LUI ($p < 0.01$) and distance from roads (D_road) ($p < 0.01$) and positively correlated with land formation time (Land_Year) ($p < 0.01$) and distance from water bodies (D_water) ($p < 0.01$). The distance from buildings had no effect on the TDGV in Lingang New City ($p < 0.05$).

To determine and compare the degree of influence of each factor on TDGV, standardized autocorrelation GLS was used (Table 4). The model equation was m5 < − gls (log(green + 1) ~scale(LUI) + scale(Land_Year) + scale (log(D_water + 1)) + scale(log(D_road + 1)), correlation = corRatio (form = ~X + Y, nugget = T), data = d2) > summary(m5).

The regression coefficients from the standardized GLS indicated that the TDGV in Lingang New City was significantly positively correlated with LUI, distance from roads (D_road), and distance from water bodies (D_water)

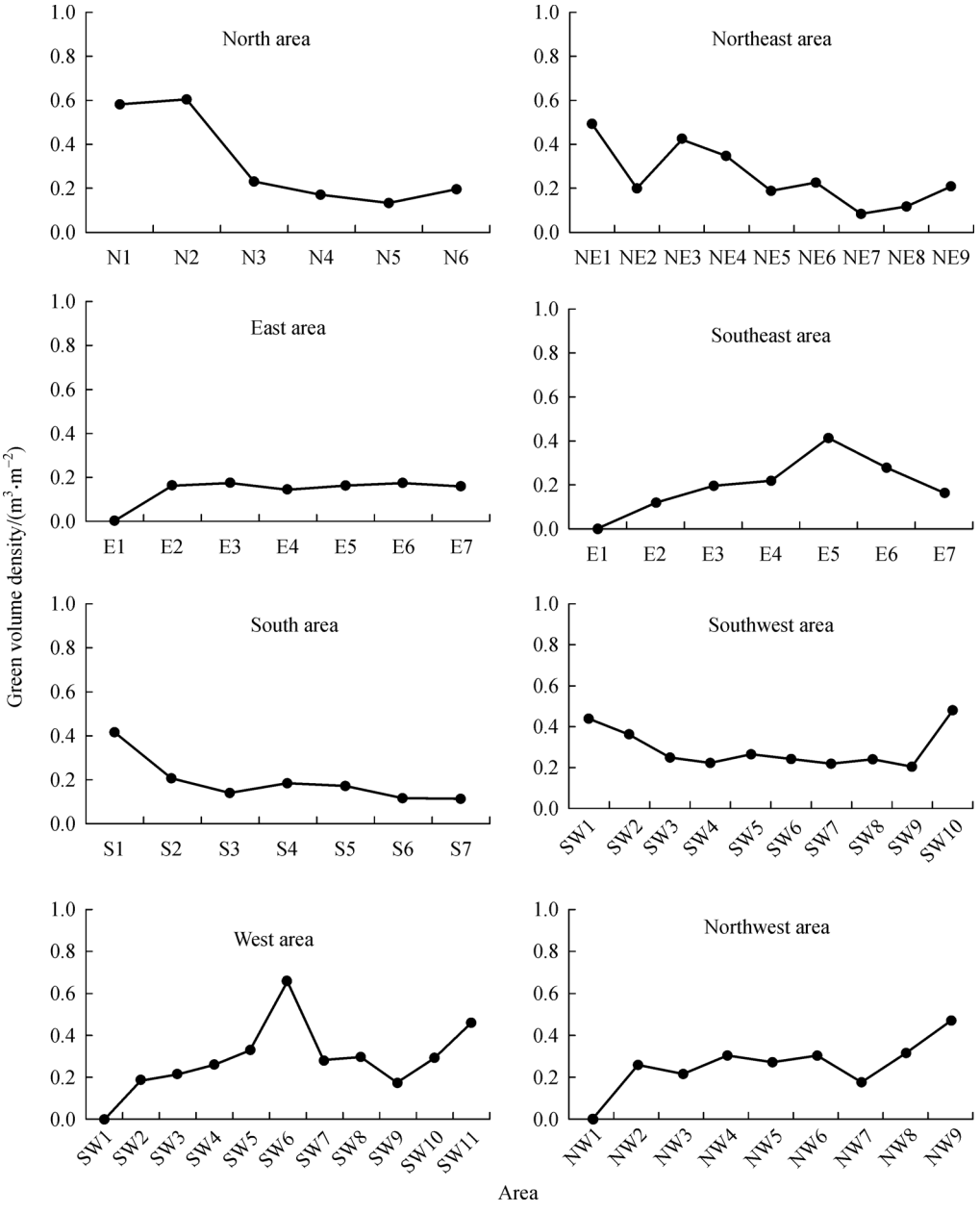

Fig. 5 Trends in three-dimensional green volume per unit area in eight transect belts with Dishui Lake at the center.

($p < 0.01$). The degree of influence decreased in the following order: distance from water (D_water) > land formation time (Land_Year) > distance from roads (D_road) > LUI (Table 5).

The GLS analysis of the TDGV values of the sample cells (100 m × 100 m) and the influencing factors showed that TDGV was affected by LUI, land formation time, and distances from roads and water bodies. Lower TDGV values were detected in areas characterized by higher LUI and lower distances from roads, which is consistent with findings from other cities and conclusions regarding the effects of rapid urbanization on urban green spaces (Liu and Liu, 2011; Nor et al., 2017; Xiong and Dai, 2017). These results reflect the strong influences of the overall planning and construction of Lingang New City on the quality and spatial pattern of its regional ecological space (Zhu et al., 2013). Higher TDGV values were observed in areas with earlier land formation times and shorter distances from water.

Under the strict adherence to the planning objectives and layout of a low-carbon city or eco-city, the values and spatial distribution of TDGV in coastal areas are affected by human interference via rapid urbanization. However, coastal reclamation areas are different from inland cities because their land resources are obtained from embankments (i.e., sea reclamation), and the natural conditions

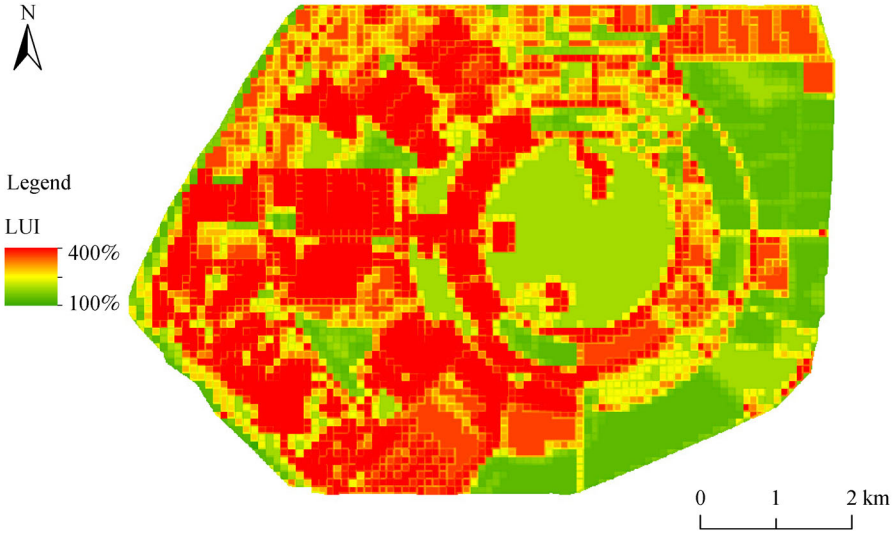

Fig. 6 Spatial distribution of LUI in Lingang New City, Shanghai.

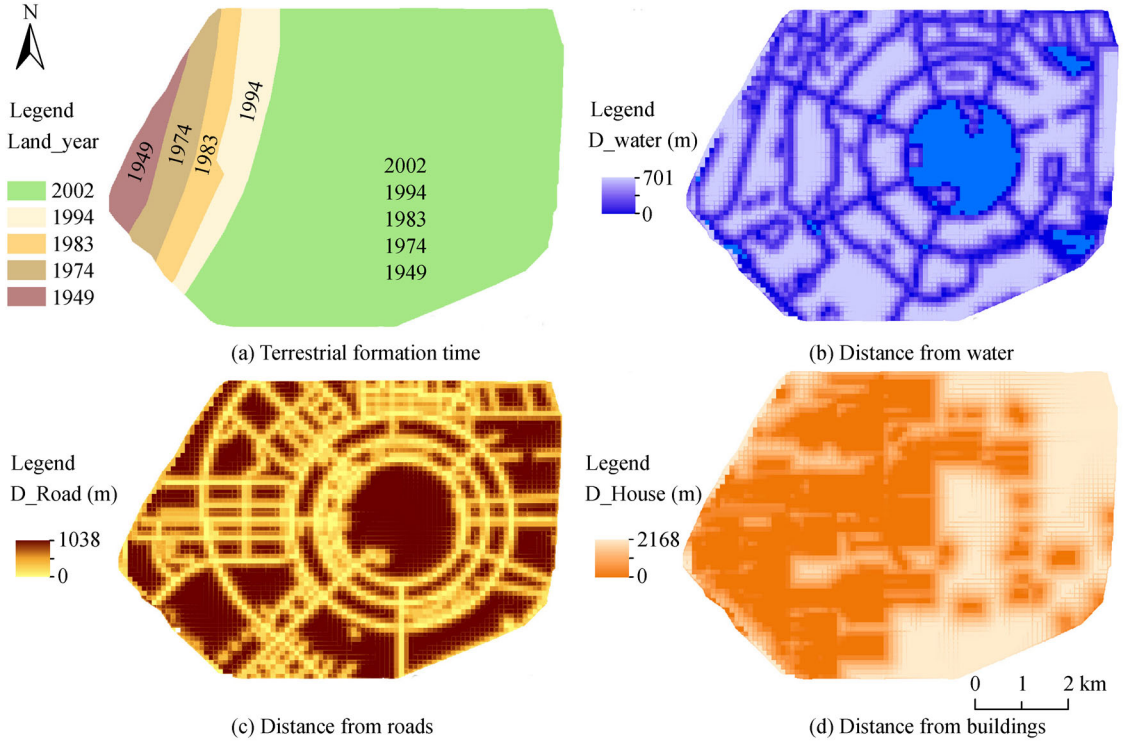

Fig. 7 Spatial distribution of patch distances from buildings, roads and water in Lingang New City, Shanghai.

Table 2 Statistical results for the optimal model

AIC	logLik	Range	Nugget	Degrees of freedom
15896.73	−7939.36	281.08	0.028	5186

Table 3 Regression coefficients of the optimal model

	Value	Std. Error	*t*-value	*p*-value
(Intercept)	5.912874	0.28438128	20.792065	0
LUI	−0.106673**	0.0380966	−2.800057	0.0051
Land_Year	0.042955**	0.0048025	8.944345	0
log(D_water + 1)	0.51576**	0.02348222	21.963852	0
log(D_road + 1)	−0.378231**	0.02545828	−14.856899	0
log(D_house + 1)	−0.005438	0.02273008	−0.239255	0.8109

Note: * $p < 0.05$, ** $p < 0.01$.

Table 4 Standardized GLS model results

AIC	logLik	Range	Nugget	Degrees of freedom
15884.97	−7934.48	199.96	0.21	5186

Table 5 Regression coefficients of the standardized GLS model

	Value	Std. Error	*t*-value	*p*-value
(Intercept)	7.039121	0.1592458	44.20287	0
scale(LUI)	−0.096466	0.03562694	−2.70768	0.0068
scale(Land_Year)	0.516165	0.05769519	8.94640	0
scale(log(D_water + 1)	0.909142	0.04004476	22.70315	0
scale(log(D_road + 1)	−0.459215	0.03113147	−14.75084	0

affected by land formation from embankments and the water distribution are also important factors that determine regional TDGV values. The time since reclamation has a profound impact on the local soil quality (Li et al., 2006), and the distribution of water bodies affects the variations in vegetation biomass in green spaces (Xenakis et al., 2012; He and Zhang, 2019). In the present study, the analysis of the main influencing factors showed that the TDGV in Lingang New City was primarily affected by land formation time and layout of the water body; that is, TDGV characteristics were affected mainly by natural soil and water factors in this coastal area. This finding differs from previous research results suggesting the effects of urbanization on TDGV. Overall, the TDGV of this coastal city is restricted by land formation time; the addition of a dense water network could increase the urban TDGV and its service efficiency, whereas the construction of a dense road network would reduce them (Fu et al., 2010; Xiong and Dai, 2017).

4 Conclusions

1) The spatial pattern of TDGV in this new coastal city showed obvious axial variations consistent with the timing of urban planning and construction, LUI and the history of regional land formation.

2) The spatial pattern of TDGV was jointly affected by anthropogenic factors and natural factors. TDGV was significantly negatively correlated with regional LUI and road network density and significantly positively correlated with regional land formation time and water network density. Because of the specific geography of this coastal area, the dominant factors affecting the spatial pattern of TDGV in this new city were two natural factors: the regional land formation time and the density of the water network.

3) TDGV evaluations can reveal the influences of anthropogenic and natural factors on the quality of urban ecological space in urban areas. TDGV could be an aspect of the monitoring of low-carbon cities, ecological urban planning and urban construction management to improve the rationality and accuracy of urban spatial layouts and land use.

Acknowledgements This work was supported by the National Key R&D Program of China (No. 2016YFC0502704) and Shanghai Key Laboratory for Urban Ecological Processes and Eco-Restoration (No. SHUES2018B07). The authors are grateful for constructive comments from Li Junxiang (Shanghai Jiaotong University) and Zhang Chao (East China Normal University).

References

Anderson K, Hancock S, Casalegno S, Griffiths A, Griffiths D, Sargent F, McCallum J, Cox D T C, Gaston K J (2018). Visualising the urban

green volume: exploring LiDAR voxels with tangible technologies and virtual models. Landsc Urban Plan, 178: 248–260

Casalegno S, Anderson K, Cox D T C, Hancock S, Gaston K J (2017). Ecological connectivity in the three-dimensional urban green volume using waveform airborne lidar. Sci Rep, 7(1): 45571

Çetin M (2016). Sustainability of urban coastal area management: a case study on Cide. J Sustain For, 35(7): 527–541

Chen P, Chu Y, Gu F X, Zhang Y D, Pan X L (2003). Spatial heterogeneity analysis of vegetation and soil characteristics in oasis-desert transition zone landscape. J Appl Ecol, 14(6): 904–908 (in Chinese)

Chunwate B T, Yahaya S, Samaila I K, Ja'afaru S W (2019). Analysis of urban land use and land cover change for sustainable development: a case of Lafia, Nasarawa State, Nigeria. J Geogr Inf Syst, 11(03): 347–358

Xenakis G, Ray D, Maurizio M (2012). Effects of climate and site characteristics on Scots pine growth. Eur J For Res, 131(2): 427–439

Fahmy M, Mahdy M, Mahmoud S, Abdelalim M, Ezzeldin S, Attia S (2020). Influence of urban canopy green coverage and future climate change scenarios on energy consumption of new sub-urban residential developments using coupled simulation techniques: a case study in Alexandria, Egypt. Energy Rep, 6(1): 638–645

Fu W, Liu S, Degloria S D, Dong S, Beazley R (2010). Characterizing the "frag-mentation–barrier" effect of road networks on landscape connectivity: a case study in Xishuangbanna, southwest China. Landsc Urban Plan, 95(3): 122–129

Gao Z Q, Liu X Y, Ning J C, Lu Q S (2014). Remote sensing based on the change and genesis of China's coastline and reclamation area in the past 30 years. Trans Chinese Soc Agr Eng, 30(12): 140–147 (in Chinese)

Gao Z Q, Liu J Y, Zhuang D F (1999). Research on land use/land cover in China based on remote sensing and GIS. National Remote Sens Bull, 3(2): 134–138 (in Chinese)

Gong J Z, Xia B C (2006). Internal structure and temporal and spatial variation of vegetation coverage in Guangzhou based on remote sensing images. J Plant Res Environ, 15(4): 25–29 (in Chinese)

Grafius D R, Corstanje R, Warren P H, Evans K L, Hancock S, Harris J A (2016). The impact of land use/land cover scale on modelling urban ecosystem services. Landsc Ecol, 31(7): 1509–1522

Gregg J W, Jones C G, Dawson T E (2003). Urbanization effects on tree growth in the vicinity of New York City. Nature, 424(6945): 183–187

Han Z L, Meng Q Q, Yan X L, Zhao W Z (2020). Spatial-temporal relationship between land use intensity and ecosystem Service value in northern Liaodong Bay in recent 30 years. Acta Ecol Sin, 2020, 40 (08): 1–12 (in Chinese)

He L S, Zhang C (2019). Influence factor analysis of Yunnan pine forest accumulation. J Southwest For U (Natural Sciences), 39(6): 116–122 (in Chinese)

Li W, Jia B Q, Wang C (2008). Research status and prospect of three dimensional green quantity of urban forest. World For Res, 21(4): 31–34 (in Chinese)

Li W J, Yu Q S (2013). Summary of history, present situation and management policy of reclamation in China. China Territory Today, (01): 36–38 (in Chinese)

Li Y, Shi Z, Jin H M, Li H Y, Wang R C (2006). Spatial variation and dynamic change of soil characteristics in reclamation area of sea floor. Bull Sci Tech, 22(6): 827–833 (in Chinese)

Liu C, Liu Z G (2011). Three-dimensional green planning analysis of Harbin urban forest based on AHP. J Northeast For U, 39(4): 52–55,129 (in Chinese)

Liu C, Xu P, Ma J (2012). Low carbon planning and target management of Shanghai Lingang New City Center. City Plan Rev, 36(12): 52–59 (in Chinese)

Ma L B, Li X Y, Cheng W J (2019). Spatial and temporal difference identification of land use intensity and its influencing factors based on irrigated area panel data. Chinese J Ecol, 38(3): 908–918 (in Chinese)

Nor A N M, Corstanje R, Harris J A, Brewer T (2017). Impact of rapid urban expansion on green space structure. Ecol Indic, 81: 274–284

Ong B L (2003). Green plot ratio: an ecological measure for architecture and urban planning. Landsc Urban Plan, 63(4): 197–211

Shanghai Urban Planning and Design Reasearch Institute (2009). Overall planning of Lingang New City. Shanghai Urban Plan Rev, (04): 11–26 (in Chinese)

Sun Q (2011). Exploration and practice of low-carbon city planning of Lingang New City. Shanghai Urban Plan Rev, (05): 24–29 (in Chinese)

Wang G, Liao S (2006). Spatial heterogeneity of land use intensity change. J Appl Ecol, 17(4): 611–614 (in Chinese)

Xiong X H, Dai Z Y (2017). Correlation analysis between ecological services and land use intensity in Fenghua City. Geospat Inform, 15 (4): 102–104 (in Chinese)

Yaralioğlu İpek, Ozden Ozge (2019). Sustainable development of urban coastal area in urban planning

Zhang L, Chen Y, Wang S T, Men M X, Xu H M (2015). Assessment and early warning of land ecological security in rapidly urbanizing coastal area: a case study of Caofeidian new district, Hebei, China. J Appl Ecol, 26(08): 2445–2454 (in Chinese)

Zhang Q, Cui X H, Xia L, Zhu Y, Zhang Q F (2008). Vegetation and soil characteristics in the embankment area of Lingang New City in Shanghai in the past 60 years. J Zhejiang For College, 25(06): 698–704 (in Chinese)

Zhou J H (2001). Urban green quantity measurement model and information system. Acta Geogr Sin, 56(1): 14–23 (in Chinese)

Zhou J H, Huang Y, Yu B L (2015). Mapping vegetation-covered urban surfaces using seeded region growing in Visible-NIR Air Photos. IEEE J-STARS, 8(5): 2212–2221

Zhou J H, Qin J, Gao K, Leng H B (2016). SVM-based soft classification of urban tree species using very high-spatial resolution remote-sensing imagery. Int J Remote Sens, 37(11): 2541–2559

Zhu S M, Hou J, Hu C H, Ding Y S (2013). Analysis of dynamic Changes of landscape Pattern of Shanghai New Port City. Geospat inform, 11(06): 106–108 + 11 (in Chinese)

Zhou T G, Luo H X, Guo D Z (2005). Quantitative research on three-dimensional green quantity of urban space based on remote sensing image. Chinese J Ecol, 25(03): 415–420 (in Chinese)

Zhou Y F, Zhou J H (2001). Evaluation system of urban ecological environment based on three-dimensional greening quantity. Chinese Landsc Architecture, 17(5): 77–79 (in Chinese)

Zhou Y F, Zhou J H (2006). Green quantity rapid measurement model. Acta Ecol Sin, 26(12): 4204–4211 (in Chinese)